

H₂-CO₂ polymer electrolyte fuel cell that generates power while evolving CH₄ at the Pt_{0.8}Ru_{0.2}/C cathode

Shofu Matsuda

Nagaoka University of Technology

Yuuki Niitsuma

Nagaoka University of Technology

Yuta Yoshida

Nagaoka University of Technology

Minoru Umeda (✉ mumeda@vos.nagaokaut.ac.jp)

Nagaoka University of Technology

Research Article

Keywords: electric power, carbon capture and utilization (CCU) strategy.

Posted Date: December 18th, 2020

DOI: <https://doi.org/10.21203/rs.3.rs-123986/v1>

License:  This work is licensed under a Creative Commons Attribution 4.0 International License.

[Read Full License](#)

Version of Record: A version of this preprint was published at Scientific Reports on April 16th, 2021. See the published version at <https://doi.org/10.1038/s41598-021-87841-4>.

Abstract

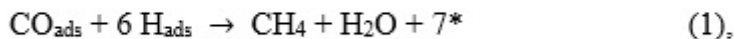
Generating electric power using CO₂ as a reactant is challenging because the electroreduction of CO₂ usually requires a large overpotential. Herein, we report the design and development of a polymer electrolyte fuel cell driven by feeding H₂ and CO₂ to the anode (Pt/C) and cathode (Pt_{0.8}Ru_{0.2}/C), respectively, based on their theoretical electrode potentials. Pt-Ru/C is a promising electrocatalysts for CO₂ reduction at a low overpotential; consequently, CH₄ is continuously produced through CO₂ reduction with an enhanced faradaic efficiency (18.2%) and without an overpotential (at 0.20 V vs. RHE) was achieved when dilute CO₂ is fed at a cell temperature of 40 °C. Significantly, the cell generated electric power (0.14 mW·cm⁻²) while simultaneously yielding CH₄ at 86.3 μmol·g⁻¹·min⁻¹. These results show that a H₂-CO₂ fuel cell is a promising technology for promoting the carbon capture and utilization (CCU) strategy.

Introduction

Recently, carbon capture and utilization (CCU) methods have received significant levels of attention as technologies for effectively removing and utilizing atmospheric CO₂¹⁻². These technologies are attractive approaches as they treat CO₂ as an unused resource and convert it into value-added chemicals and fuels. Among them, electroreduction is a promising technique, and C₁, C₂, and C₂₊ products have reportedly been obtained using various electrocatalysts through different CO₂ reduction mechanisms³⁻¹³. In particular, CO production at Au and Ag, and hydrocarbon production at Cu, have been successfully elucidated to follow multistep proton-coupled electron-transfer pathways^{14,15}. These reactions exhibit relatively high faradaic efficiencies; however, they require large overpotentials, which is disadvantageous. Consequently, their energy-conversion efficiencies are low, despite their high faradaic efficiencies.

Developing methods that ensure that the CO₂-electroreduction reaction occurs with a small overpotential and a high energy-conversion efficiency is important. In this regard, platinum group metals have the potential to realize overpotential-free CO₂ reductions. There are many reports in which CO is adsorbed on a metal (CO_{ads}) at a positive potential rather than its theoretical potential^{16,17}. However, the further reduction of CO_{ads} is difficult because CO is strongly adsorbed to the metal through a donation–back-donation mechanism (Blyholder mechanism)¹⁸. To the best of our knowledge, the main product is H₂ when a Pt electrocatalyst is used, even when it is negatively polarized¹⁹⁻²¹. We previously obtained the C1 compound by reducing CO₂ near the theoretical potential in a proton-exchange-type membrane electrode assembly (MEA) with a carbon-supported platinum (Pt/C) electrocatalyst²². The use of a proton-exchange membrane and an ionomer was suggested to facilitate CO₂ reduction; however, the C1 yield was quite low. We recently demonstrated that CH₄ can be produced by the reduction of CO₂ in the absence of an overpotential and with a faradaic efficiency of 6.8% using the MEA²³. This CH₄-generation

reaction proceeds by a Langmuir–Hinshelwood (L-H) mechanism associated with CO_{ads} and H adsorbed on the metal (H_{ads}):



where * represents an active site on the metal catalyst. It follows that placing CO_{ads} and H_{ads} in the appropriate ratio on the metal surface is important for CH_4 production, and this is realized by controlling the CO_2 -feed concentration as well as the electrode potential in the case of a Pt catalyst²⁴. Based on these techniques, we reported CO_2 reduction at a Pt catalyst to generate CH_4 with a faradaic efficiency of 12.3% at 0.16 V vs. RHE using 4 vol% CO_2 diluted with Ar (ref²⁵).

Here, the most noteworthy point is that the CH_4 -synthesis potential is almost the same as the theoretical potential, which is more positive than that for the hydrogen oxidation reaction (HOR). Therefore, power can be generated by an H_2 - CO_2 fuel cell²⁶ by combining the HOR and the CO_2 reduction reaction (to generate CH_4) as the anodic and cathodic reactions, respectively²⁵. The H_2 - CO_2 fuel cell is a promising CCU technology that utilizes CO_2 as a resource to generate electricity while producing a valuable compound (CH_4). However, the CH_4 yield as well as the amount of power generated need to be increased to further develop this technology, and the efficient use of CO_{ads} , which requires weakening the CO-metal bond, would represent a potential breakthrough toward this goal.

Pt-Ru alloy catalysts are known to impact the ligand effect, in which Ru affects the electronic state of CO_{ads} and weakens the CO-metal bond²⁷⁻³⁰. In our previous study, we investigated the reduction of CO_2 using MEAs incorporated with Pt-Ru electrocatalysts and revealed that the CH_4 -generation efficiencies at the theoretical potential follow the order: Pt/C < $\text{Pt}_{0.5}\text{Ru}_{0.5}$ /C < $\text{Pt}_{0.8}\text{Ru}_{0.2}$ /C when 100 vol% CO_2 was supplied³¹. For this reason, we expected that CH_4 would be more-efficiently produced by the reduction of CO_2 without an overpotential by combining both techniques, namely diluting the CO_2 concentration and using an MEA with the $\text{Pt}_{0.8}\text{Ru}_{0.2}$ /C electrocatalyst. In this work, we designed a polymer electrolyte fuel cell that incorporated an MEA with a $\text{Pt}_{0.8}\text{Ru}_{0.2}$ /C cathode and a Pt/C anode. This paper reports the reduction of CO_2 for the simultaneous production of CH_4 and power by supplying CO_2 and H_2 to the cathode and anode, respectively.

Results

Effect of CO_2 concentration on CH_4 yield

We first performed cyclic voltammetry (CV) to assess the cathodic reaction of the prepared cell (Fig. 1a) under various CO₂ concentrations in Ar at a cell temperature of 40 °C. As shown in Fig. 1b, the oxidation current decreases with increasing CO₂ concentration in the 0.08–0.43 V (vs. RHE) potential range, whereas it increases between 0.43 and 0.70 V (vs. RHE). Considering that the former and the latter are the oxidation currents that originate from H desorption and CO desorption, respectively³², this result reveals that the amounts of CO_{ads} and H_{ads} increase and decrease, respectively, with increasing CO₂ concentration. The faradaic charges calculated from Fig. 1b are shown in Fig. 1c, in which a trade-off relationship between the faradaic charges for CO_{ads} (Q_{CO}) and H_{ads} (Q_H) are clearly observed. Therefore, the amounts of CO_{ads} and H_{ads} on the Pt_{0.8}Ru_{0.2}/C catalyst surface can be controlled by changing the concentration of CO₂ supplied to the cathode. The onset potential for CO_{ads} desorption was determined, as shown by the black arrow in Fig. 1b, which provided a value of 0.43 V (vs. RHE) for Pt_{0.8}Ru_{0.2}/C, which is more negative than that for Pt/C (0.45 V vs. RHE²⁵), suggesting that the Pt_{0.8}Ru_{0.2}/C electrocatalyst exhibits a lower CO-adsorption energy.

CH₄ generation from CO₂ reduction at the Pt_{0.8}Ru_{0.2}/C electrocatalyst was next investigated. Figures 2a and 2b show cyclic voltammograms with in-line MS signals (m/z 2 and 15) at CO₂ concentrations of 7 vol% and 100 vol%, respectively. The signal at m/z 15 was simultaneously detected with a reduction current at 7 vol% CO₂ when the potential was below ~ 0.25 V (vs. RHE), whereas the m/z 15 signal only was weakly detected at 100 vol% CO₂. The pattern in the mass spectrum of the cathodic output gas from the cell at 0.10 V (vs. RHE) in the 7 vol% CO₂ atmosphere (Supplementary Fig. S1) is concordant with that of the CH₄ standard gas; hence, the detected signal at m/z 15, which corresponds to CH₃⁺ (not affected by H₂O and CO₂), is entirely derived from CH₄ produced through the reduction of CO₂. It should be noted that the signal at m/z 2 as hydrogen generation started to be detected at ~ 0.08 V (vs. RHE) at all CO₂ concentrations. Figure 2c shows the dependence of the faradaic efficiency determined during CH₄ generation on the CO₂ concentration acquired during negative-potential-sweep CV between 0.20 and 0.10 V (vs. RHE). The faradaic efficiency was determined as a percentage of the methanogenic faradaic charge relative to the total faradaic charge. As a result, the highest faradaic efficiency of ~ 4.5% was calculated at 7 vol% CO₂, which exceeds the efficiency for Pt/C (3.0% in a 5 vol% CO₂ atmosphere²⁴). On the other hand, the faradaic efficiency was only 0.61% in 100 vol% CO₂, which corresponds to our previously reported efficiency³¹. Overall, we determined 7 vol% to be the preferred CO₂ concentration for generating CH₄ at the Pt_{0.8}Ru_{0.2}/C electrocatalyst.

CH₄-generation dependence on the CO₂ electroreduction potential

We next explored the optimum potential for CH₄ production at the Pt_{0.8}Ru_{0.2}/C electrocatalyst with the supplied CO₂ concentration fixed at 7 vol%. The cathode potential was stepped 14 times in the negative direction in the 0.40–0.05 V (vs. RHE) range every 2 min. As shown in Fig. 3a, which was produced by analyzing Supplementary Fig. S2, the signal at m/z 15 for CH₄ began to be detected at 0.30 V (vs. RHE), was most intense at around 0.20 V (vs. RHE), and began to decrease in intensity below this value.

Meanwhile, the signal at m/z 2 for H_2 was observed only at 0.08 V and 0.05 V (vs. RHE), where CH_4 generation was suppressed. These results reveal that CH_4 production occurs at a more positive potential than H_2 evolution, with a maximum CH_4 yield observed at 0.20 V (vs. RHE). The in-line MS signals (m/z 2 and 15) recorded during cyclic voltammetry at 0 vol% CO_2 (100 vol% Ar) shown in Supplementary Fig. S3 reveal that the m/z 15 signal was hardly detected at all cathode potentials. Based on the standard $CO_2|CH_4$ electrode potential (0.169 V vs. SHE³³), we successfully generated CH_4 from CO_2 in the absence of an overpotential in this study. Therefore, from the viewpoints of CH_4 yield and product selectivity, 0.20 V vs. RHE was determined to be the preferred potential.

We subsequently directly stepped the potential from 0.40 V to 0.20 V (vs. RHE). As shown in Fig. 3b, the intensity of the m/z 15 signal was observed to be almost constant when the potential was held at 0.20 V (vs. RHE). Supplementary Fig. S4 shows gas chromatograms of the cathodic output gas from the cell in which the cathode potential was held at 0.20 V (vs. RHE). Based on the results obtained using flame-ionization and thermal-conductivity detectors, only CH_4 was produced during CO_2 reduction at $Pt_{0.8}Ru_{0.2}/C$. Significantly, the faradaic efficiency was calculated to be 18.2% between 240 s and 299 s in Fig. 3b, which exceeds the previously reported Pt/C efficiency (12.3%²⁵). Overall, continuous CH_4 generation with enhanced efficiency and zero overpotential was achieved at a CO_2 concentration of 7 vol% and a holding potential of 0.20 V (vs. RHE).

Power generation as an H_2 - CO_2 fuel cell

Figure 4 shows power generation characteristics as well as CH_4 -production rates determined from the data in Fig. 3a, which reveals that the power density (as an H_2 - CO_2 fuel cell) and the CH_4 yield rate exhibit similar trends, with maximum values of $\sim 0.14 \text{ mW}\cdot\text{cm}^{-2}$ and $86.3 \text{ }\mu\text{mol}\cdot\text{g}^{-1}\cdot\text{min}^{-1}$, respectively, at a cell voltage of 0.20 V. Compared to a report on the formation of CH_3OH (but not CH_4) through CO_2 reduction at Pt-Ru/C using an MEA³⁴, the rate of CH_4 production in this study is higher.

Finally, we compared the results obtained for $Pt_{0.8}Ru_{0.2}/C$ with those for Pt/C. As listed in Table 1, the power density, CH_4 yield rate, and faradaic efficiency were ~ 10 -, ~ 3.5 -, and ~ 1.5 -times higher, respectively, when the $Pt_{0.8}Ru_{0.2}/C$ electrocatalyst was used instead of the Pt/C electrocatalyst. Therefore, we demonstrated a H_2 - CO_2 fuel cell that generates electric power while efficiently reducing CO_2 to CH_4 .

Table 1
Comparing Pt_{0.8}Ru_{0.2}/C and Pt/C cathode electrocatalyst data for the H₂-CO₂ fuel cell. Pt/C data are taken from our previous report²⁵.

	Pt _{0.8} Ru _{0.2} /C	Pt/C
Cell voltage / V	0.20	0.16
Power density / mW cm ⁻²	0.14	0.015
CH ₄ yield rate / μmol g ⁻¹ h ⁻¹	86.3	26.4
Faradaic efficiency / %	18.2	12.3

Discussion

In the present study, we designed and demonstrated an H₂-CO₂ polymer-electrolyte fuel cell that generates CH₄ from CO₂ with enhanced efficiency, which was achieved by the strategic use of a Pt_{0.8}Ru_{0.2}/C cathodic catalyst. As mentioned in the introduction, the generation of CH₄ through the reduction of CO₂ follows the L-H mechanism involving CO_{ads} and H_{ads} (ref²³). According to equation (1), this reaction theoretically proceeds at a CO_{ads}-to-H_{ads} molar ratio of 1:6; however, this reaction proceeded when the ratio was 1:11 or higher for a Pt/C electrocatalyst²⁴, with the best ratio reported to be 1:18 (ref²⁴). On the other hand, this ratio at the Pt_{0.8}Ru_{0.2}/C electrocatalyst was determined to be 1:8 at a CO₂ concentration of 7 vol% according to the following equation:

$$\text{CO}_{\text{ads}} : \text{H}_{\text{ads}} = \left(\frac{Q_{\text{CO}}}{2}\right) : Q_{\text{H}}. \quad (2).$$

Hence, CO_{ads} can be used to efficiently generate CH₄ at Pt_{0.8}Ru_{0.2}/C because the ratio is close to the theoretical value of 1:6, which leads to a higher faradaic CH₄-production efficiency, and was achieved by the lower CO-adsorption energy associated with the Pt_{0.8}Ru_{0.2}/C electrocatalyst.

The sustained generation of CH₄ at 0.20 V (vs. RHE) (Fig. 3b) is also related to the CO_{ads}-to-H_{ads} ratio. Based on Supplementary Fig. S5, this ratio was determined to be 1:7 after holding at a potential of 0.20 V (vs. RHE) for 5 min at 7 vol% CO₂. Therefore, CH₄ is continuously generated at Pt_{0.8}Ru_{0.2}/C because the CO_{ads}-to-H_{ads} ratio was slightly different when the potential was held at 0.20 V (vs. RHE). It should be noted that the CH₄-production reaction proceeds at a more-positive potential than its theoretical potential. Although the reason is unclear at present, there is one possible explanation for this observation. In our system, the CO₂|CH₄ equilibrium potential is influenced by the proton activity of the Nafion membrane

electrolyte. As shown in Supplementary Fig. S3, the H₂-evolution onset potential is ~0.08 V (vs. RHE); this value does not correspond to the theoretical potential (0.00 V vs. SHE³³). In addition, the proton activity of the Nafion membrane has been reported to be different to that observed under SHE conditions³⁵⁻³⁷. Importantly, the CH₄-generation reaction is likely to occur through a sequential CO₂ CO_{ads} CH₄ reduction process, rather than through a one-step process (CO₂ CH₄). Supplementary Fig. S6 shows that the onset potential for the formation of CO_{ads} from CO₂ through reduction at Pt_{0.8}Ru_{0.2}/C in 7 vol% CO₂ is 0.375 V (vs. RHE). Hence, an electrode potential that progresses the CO_{ads} CH₄ process can drive the overall reaction.

H₂-CO₂ fuel cells function when platinum group metals are employed as cathodic catalysts. In other words, a H₂-CO₂ fuel cell does not function using “active” electrocatalysts composed of only Cu, Au, and Ag, as well as their alloys, because CO₂ reduction proceeds at a more negative potential than that for the evolution of H₂ evolution (the overpotential is large)³⁸. It should be noted that the highest faradaic CH₄-yield efficiency was only 18.2% in this study, which is insufficient for practical applications. The reason for this low efficiency has not yet been clarified; one possible process that contributes to the rest efficiency involves the formation of CO_{ads} and H_{ads}, which are not associated with CH₄ generation. Hence, further increasing the efficiency through catalyst design, including optimizing the Ru ratio in the Pt-Ru catalyst, will be important. One significant advantage of this technology is that the CO₂-conversion reaction that produces CH₄ occurs at a lower temperature (40°C) than that used in chemical methanation technology³⁹ and CO₂-utilization technologies that rely on solid oxide electrolytes⁴⁰ and molten salts⁴¹, which require temperature of several hundreds of degrees.

In conclusion, this work provides a novel approach to H₂-CO₂ fuel cells as a CO₂-utilization technology. CH₄ is produced continuously by the reduction of CO₂ in the absence of an overpotential (at 0.20 V vs. RHE) in a cell that uses an MEA with a Pt_{0.8}Ru_{0.2}/C cathode at a CO₂ concentration of 7 vol% and a cell temperature of 40°C, and electrical energy is generated by combining the CO₂-reduction and H₂-oxidation (at a Pt/C anode) reactions. These results facilitate the carbon utilization strategy, although further investigations are necessary before it can be considered for practical applications.

Methods

Materials. Pt_{0.8}Ru_{0.2}/C (42.5 wt%; TECRuE43) and Pt/C (46.2 wt%; TEC10E50E) electrocatalyst powders were obtained from Tanaka Kikinokogyo Co., Ltd. Nafion-117 membranes (0.18-mm thick) were purchased from DuPont and boiled successively in Milli-Q water, 0.5 M H₂O₂, 0.5 M H₂SO₄, and Milli-Q water (1 h each) prior to use. All chemicals (H₂O₂, H₂SO₄, acetone, 2-propanol, methanol, and 5 wt% Nafion solution) were obtained from the Fujifilm Wako Pure Chemical Corporation. Water-repellent carbon paper (TGP-H-060H) was purchased from Toray Industries, Inc, and polymer electrolyte cell components (gasket, separator with parallel flow paths, and stainless steel plate) were purchased from Miclab.

Cell fabrication. A polymer electrolyte fuel cell (PEFC) was fabricated by essentially following the same procedure reported previously^{23–25}, with the exception that Pt_{0.8}Ru_{0.2}/C was used as the cathode instead of Pt/C. Briefly, a 6 × 6 cm Nafion 117 membrane and 3 × 3 cm pieces of carbon paper pretreated with acetone were used as the proton-exchange membrane and gas diffusion layers, respectively. The electrocatalyst dispersion was prepared by mixing the Pt_{0.8}Ru_{0.2}/C catalyst with 5 wt% Nafion (1:1 v/v) and an aqueous solution containing 1:2:1 (w/w/w) 2-propanol, methanol, and Milli-Q water, followed by spraying onto one piece carbon paper to prepare the cathode. The anode was prepared by spraying a Pt/C electrocatalyst dispersion onto another piece of carbon paper. The amount of loaded metal and the apparent electrode surface area were 1.0 mg·cm⁻² and 9.0 cm², respectively, on both electrodes. The MEA was prepared by bringing these electrodes into contact with each side of the Nafion-117 membrane, followed by hot-pressing at 140 °C with a 4.5 kN load for 10 min. It should be noted that the Pt/C electrocatalyst dispersion was dropped onto the Nafion 117 membrane on the anode side to provide a reference reversible hydrogen electrode (RHE). Finally, the MEA, gasket, separator, and stainless steel plate were assembled to complete the PEFC used in this study, as shown in Fig. 1a.

Electrochemical CO₂ reduction and product analysis. A schematic diagram of the experimental setup used in this study is shown in Fig. 1a. Electrochemical experiments were conducted using a PEFC-operating apparatus (FCG-20S, ACE), a potentiostat/galvanostat (HA-310, Hokuto Denko), and a function generator (HB-104, Hokuto Denko). Fully humidified 100 vol% H₂ and CO₂ diluted with Ar (CO₂ concentration: 0, 4, 7, 10, 20, 50, and 100 vol%) gas were fed to the anode and cathode at 50 cm³·min⁻¹, respectively, in all experiments. Fully humidified 100 vol% H₂ gas was supplied to the reference electrode at 10 cm³·min⁻¹. The cell temperature was set to 40 °C. The H₂, CO₂, and Ar gases were 99.999%, 99.995%, and 99.998% pure, respectively. The cathodic potential was scanned in the 0.08–0.70 V (vs. RHE) range at 10 mV·s⁻¹ during CV. It should be noted that a 0.05–0.70 V (vs. RHE) potential range was used for CV with in-line product analysis. In the potential-step experiment, the cathodic potential was stepped through 14 levels in the 0.40–0.05 V (vs. RHE) range in the negative direction every 2 min at a CO₂ concentration of 7 vol%. In addition, the cathodic potential was directly stepped from 0.40 to 0.20 V (vs. RHE) at 7 vol% CO₂ and held there for 5 min, after which it was stepped to 0.05 V (vs. RHE). In-line mass spectrometry (MS) was carried out during the electrochemical experiments by introducing the cathode exhaust gas directly to a mass spectrometer (JMS-Q1050GC, JEOL). The ionization voltage was 23 eV. Note that the lag time for in-line MS product detection was adjusted by the H₂ evolution response (7 s). A calibration curve, which was obtained using CH₄ gas (purity: 99.999%) diluted with Ar, was used to calculate the faradaic efficiencies and CH₄-yield rates.

Declarations

Acknowledgement

This work was supported by JSPS KAKENHI Grant Number JP20H00282.

Author contributions

M.U. conceived the idea and supervised the entire project. M.U. and S.M. designed the experiments. Y.N. and Y.Y. performed all experiments. All authors analyzed the experimental data. S.M. wrote the paper.

Additional information

Supplementary information is available for this paper at <http://...>

Competing interests: The authors declare no competing interests.

References

1. Hepburn, C. et al. The technological and economic prospects for CO₂ utilization and removal. *Nature* **575**, 87–97, DOI: <https://doi.org/10.1038/s41586-019-1681-6> (2019).
2. Abanades, J. C., Rubin, E. S., Mazzotti, M. & Herzog, H. J. On the climate change mitigation potential of CO₂ conversion to fuels. *Energy Environ. Sci.* **10**, 2491–2499, DOI: <https://doi.org/10.1039/C7EE02819A> (2017).
3. Liu, M. et al. Enhanced electrocatalytic CO₂ reduction via field-induced reagent concentration. *Nature* **537**, 382–386, DOI: <https://doi.org/10.1038/nature19060> (2016).
4. Hossain, M. H., Wen, J. & Chen., A. Unique copper and reduced graphene oxide nanocomposite toward the efficient electrochemical reduction of carbon dioxide. *Rep.* **7**, 3184, DOI: <https://doi.org/10.1038/s41598-017-03601-3> (2017).
5. Liu, S. et al. Shape-dependent electrocatalytic reduction of CO₂ to CO on triangular silver nanoplates. *Am. Chem. Soc.* **139**, 2160–2163, DOI: <https://doi.org/10.1021/jacs.6b12103> (2017).
6. Nguyen, D. L. T. et al. Selective CO₂ reduction on zinc electrocatalyst: The effect of zinc oxidation state induced by pretreatment environment. *ACS Sustainable Chem. Eng.* **5**, 11377–11386, DOI: <https://doi.org/10.1021/acssuschemeng.7b02460> (2017).
7. Li, F., Chen, L., Knowles, P. G., MacFarlane, D. R. & Zhang, J. Hierarchical mesoporous SnO₂ nanosheets on carbon cloth: a robust and flexible electrocatalyst for CO₂ reduction with high efficiency and selectivity. *Chem. Int. Ed.* **56**, 505–509, DOI: <https://doi.org/10.1002/anie.201608279> (2017).
8. Wu, Y., Jiang, Z., Lu, X., Liang, Y. & Wang, H. Domino electroreduction of CO₂ to methanol on a molecular catalyst. *Nature* **575**, 639–642, DOI: <https://doi.org/10.1038/s41586-019-1760-8> (2019).
9. Choi, J. et al. Energy efficient electrochemical reduction of CO₂ to CO using a three-dimensional porphyrin/graphene hydrogel. *Energy Environ. Sci.* **12**, 747–755, DOI: <https://doi.org/10.1039/C8EE03403F> (2019).
10. Zhang, E. et al. Bismuth single atoms resulting from transformation of metal–organic frameworks and their use as electrocatalysts for CO₂. *J. Am. Chem. Soc.* **141**, 16569–16573, DOI:

- <https://doi.org/10.1021/jacs.9b08259> (2019).
11. Todoroki, N., Tei, H., Tsurumaki, H., Miyakawa, T., Inoue, T. & Wadayama, T. Surface atomic arrangement dependence of electrochemical CO₂ reduction on gold: online electrochemical mass spectrometric study on low-index Au(*hkl*) Surfaces. *ACS Catal.* **9**, 1383–1388, DOI: <https://doi.org/10.1021/acscatal.8b04852> (2019).
 12. Kim, T. & Palmore, T. R. A scalable method for preparing Cu electrocatalysts that convert CO₂ into C₂+ *Nat. Commun.* **11**, 3622, DOI: <https://doi.org/10.1038/s41467-020-16998-9> (2020).
 13. Arán-Ais, R. M. et al. Imaging electrochemically synthesized Cu₂O cubes and their morphological evolution under conditions relevant to CO₂ *Nat. Commun.* **11**, 3489, DOI: <https://doi.org/10.1038/s41467-020-17220-6> (2020).
 14. Kortlever, R., Shen, J., Schouten, K. J. P., Calle-Vallejo, F. & Koper, M. T. M. Catalysts and reaction pathways for the electrochemical reduction of carbon dioxide. *Phys. Chem. Lett.* **6**, 4073–4082, DOI: <https://doi.org/10.1021/acs.jpcllett.5b01559> (2015).
 15. Peterson, A. A., Abild-Pedersen, F., Studt, F., Rossmeisl, J. & Nørskov, J. K. How copper catalyzes the electroreduction of carbon dioxide into hydrocarbon fuels. *Energy Environ. Sci.* **3**, 1311–1315, DOI: <https://doi.org/10.1039/C0EE00071J> (2010).
 16. Giner, J. Electrochemical reduction of CO₂ on platinum electrodes in acid solutions. *Acta* **8**, 857–865, DOI: [https://doi.org/10.1016/0013-4686\(63\)80054-7](https://doi.org/10.1016/0013-4686(63)80054-7) (1963).
 17. Hori, Y. Electrochemical CO₂ reduction on metal electrodes. *Aspects Electrochem.* **42**, 89–189, DOI: https://doi.org/10.1007/978-0-387-49489-0_3 (2008).
 18. Koper, M. T. M. & van Santen, R. A. Electric field effects on CO and NO adsorption at the Pt(111) surface. *Electroanal. Chem.* **476**, 64–70, DOI: [https://doi.org/10.1016/S0022-0728\(99\)00367-8](https://doi.org/10.1016/S0022-0728(99)00367-8) (1999).
 19. Hori, Y., Wakebe, H., Tsukamoto, T. & Koga, O. Electrocatalytic process of CO selectivity in electrochemical reduction of CO₂ at metal electrodes in aqueous media. *Acta* **39**, 1833–1839, DOI: [https://doi.org/10.1016/0013-4686\(94\)85172-7](https://doi.org/10.1016/0013-4686(94)85172-7) (1994).
 20. Kuhl, K. P., Hatsukade, T., Cave, E. R., Abram, D. N., Kibsgaard, J. & Jaramillo, T. F. Electrocatalytic conversion of carbon dioxide to methane and methanol on transition metal surfaces. *Am. Chem. Soc.* **136**, 14107–14113, DOI: <https://doi.org/10.1021/ja505791r> (2014).
 21. Lee, J., Lim, J., Roh, C.-W., Whang, H. S. & Lee, H. Electrochemical CO₂ reduction using alkaline membrane electrode assembly on various metal electrodes. *CO₂ Util.* **31**, 244–250, DOI: <https://doi.org/10.1016/j.jcou.2019.03.022> (2019).
 22. Shironita, S., Karasuda, K., Sato, M. & Umeda, M. Feasibility investigation of methanol generation by CO₂ reduction using Pt/C-based membrane electrode assembly for a reversible fuel cell. *Power Sources* **228**, 68–74, DOI: <https://doi.org/10.1016/j.jpowsour.2012.11.097> (2013).
 23. Umeda, M., Niitsuma, Y., Horikawa, T., Matsuda, S. & Osawa, M. Electrochemical reduction of CO₂ to methane on platinum catalysts without overpotentials: strategies for improving conversion

- efficiency. *ACS Appl. Energy Mater.* **3**, 1119–1127, DOI: <https://doi.org/10.1021/acsaem.9b02178> (2020).
24. Matsuda, S., Tamura, S., Yamanaka, S., Niitsuma, Y., Sone, Y. & Umeda, M. Minimization of Pt-electrocatalyst deactivation in CO₂ reduction using a polymer electrolyte cell. *Chem. Eng.* **5**, 1064–1070, DOI: <https://doi.org/10.1039/d0re00083c> (2020).
25. Umeda, M., Yoshida, Y. & Matsuda, S. Highly selective methane generation by carbon dioxide electroreduction on carbon-supported platinum catalyst in polymer electrolyte fuel cell. *Acta* **340**, 135945, DOI: <https://doi.org/10.1016/j.electacta.2020.135945> (2020).
26. Umeda, M., Sato, M., Maruta, T. & Shironita, S. Is power generation possible by feeding carbon dioxide as reducing agent to polymer electrolyte fuel cell? *Appl. Phys.* **114**, 174908, DOI: <https://doi.org/10.1063/1.4829030> (2013).
27. Waszczuk, P. et al. Adsorption of CO poison on fuel cell nanoparticle electrodes from methanol solutions: a radioactive labeling study. *Electroanal. Chem.* **511**, 55–64, DOI: [https://doi.org/10.1016/S0022-0728\(01\)00559-9](https://doi.org/10.1016/S0022-0728(01)00559-9) (2001).
28. Christoffersen, E., Liu, P., Ruban, A., Skriver, H. L. & Nørskov, J. K. Anode materials for low-temperature fuel cells: a density functional theory study. *Catal.* **199**, 123–131, DOI: <https://doi.org/10.1006/jcat.2000.3136> (2001).
29. Wakisaka, M., Mitsui, S., Hirose, Y., Kawashima, K., Uchida, H. & Watanabe, M. Electronic structures of Pt-Co and Pt-Ru alloys for CO tolerant anode catalysts in polymer electrolyte fuel cells studied by EC-XPS. *Phys. Chem. B* **110**, 23489–23496, DOI: <https://doi.org/10.1021/jp0653510> (2006).
30. Furukawa, H., Matsuda, S., Tanaka, S., Shironita, S. & Umeda, M. CO₂ electroreduction characteristics of Pt-Ru/C powder and Pt-Ru sputtered electrodes under acidic condition. *Surf. Sci.* **434**, 681–686, DOI: <https://doi.org/10.1016/j.apsusc.2017.10.219> (2018).
31. Niitsuma, Y., Sato, K., Matsuda, S., Shironita, S. & Umeda, M. CO₂ reduction performance of Pt-Ru/C electrocatalyst and its power generation in polymer electrolyte fuel cell. *Electrochem. Soc.* **166**, F208–F213, DOI: <https://doi.org/10.1149/2.0531904jes> (2019).
32. Shironita, S., Karasuda, K., Sato, K. & Umeda, M. Methanol generation by CO₂ reduction at a Pt-Ru/C electrocatalyst using a membrane electrode assembly. *Power Sources* **240**, 404–410, DOI: <https://doi.org/10.1016/j.jpowsour.2013.04.034> (2013).
33. Bard, A. J., Parsons, R. & Jordan, J. *Standard potentials in aqueous solution* (Marcel Dekker, Inc., New York and Basel, 1985).
34. Sebastián, D. et al. CO₂ reduction to alcohols in a polymer electrolyte membrane co-electrolysis cell operating at low potentials. *Acta* **241**, 28–40, DOI: <https://doi.org/10.1016/j.electacta.2017.04.119> (2017).
35. Seger, B., Vinodgopal, K. & Kamat, P. V. Proton activity in Nafion films: Probing exchangeable protons with methylene blue. *Langmuir* **23**, 5471–5476, DOI: <https://doi.org/10.1021/la0636816> (2007).

36. Umeda, M., Sayama, K., Maruta, T. & Inoue, M. Proton activity of Nafion 117 membrane measured from potential difference of hydrogen electrodes. *Ionics* **19**, 623–627, DOI: <https://doi.org/10.1007/s11581-012-0791-z> (2013).
37. Brightman, E. & Pasquier, D. Measurement and adjustment of proton activity in solid polymer electrolytes. *Commun.* **82**, 145–149, DOI: <https://doi.org/10.1016/j.elecom.2017.08.005> (2017).
38. Zhang, W. et al. Progress and perspective of electrocatalytic CO₂ reduction for renewable carbonaceous fuels and chemicals. *Sci.* **5**, 1700275, DOI: <https://doi.org/10.1002/adv.201700275> (2018).
39. Wang, W., Wang, S., Ma, X. & Gong, J. Recent advances in catalytic hydrogenation of carbon dioxide. *Soc. Rev.* **40**, 3703–3727, DOI: <https://doi.org/10.1039/C1CS15008A> (2011).
40. Lu, J. et al. Highly efficient electrochemical reforming of CH₄/CO₂ in a solid oxide electrolyser. *Adv.* **4**, eaar5100, DOI: <https://doi.org/10.1126/sciadv.aar5100> (2018).
41. Banerjee, A., Dick, G. R., Yoshino, T. & Kanan, M. W. Carbon dioxide utilization via carbonate-promoted C–H carboxylation. *Nature* **531**, 215–219, DOI: <https://doi.org/10.1038/nature17185> (2016).

Figures

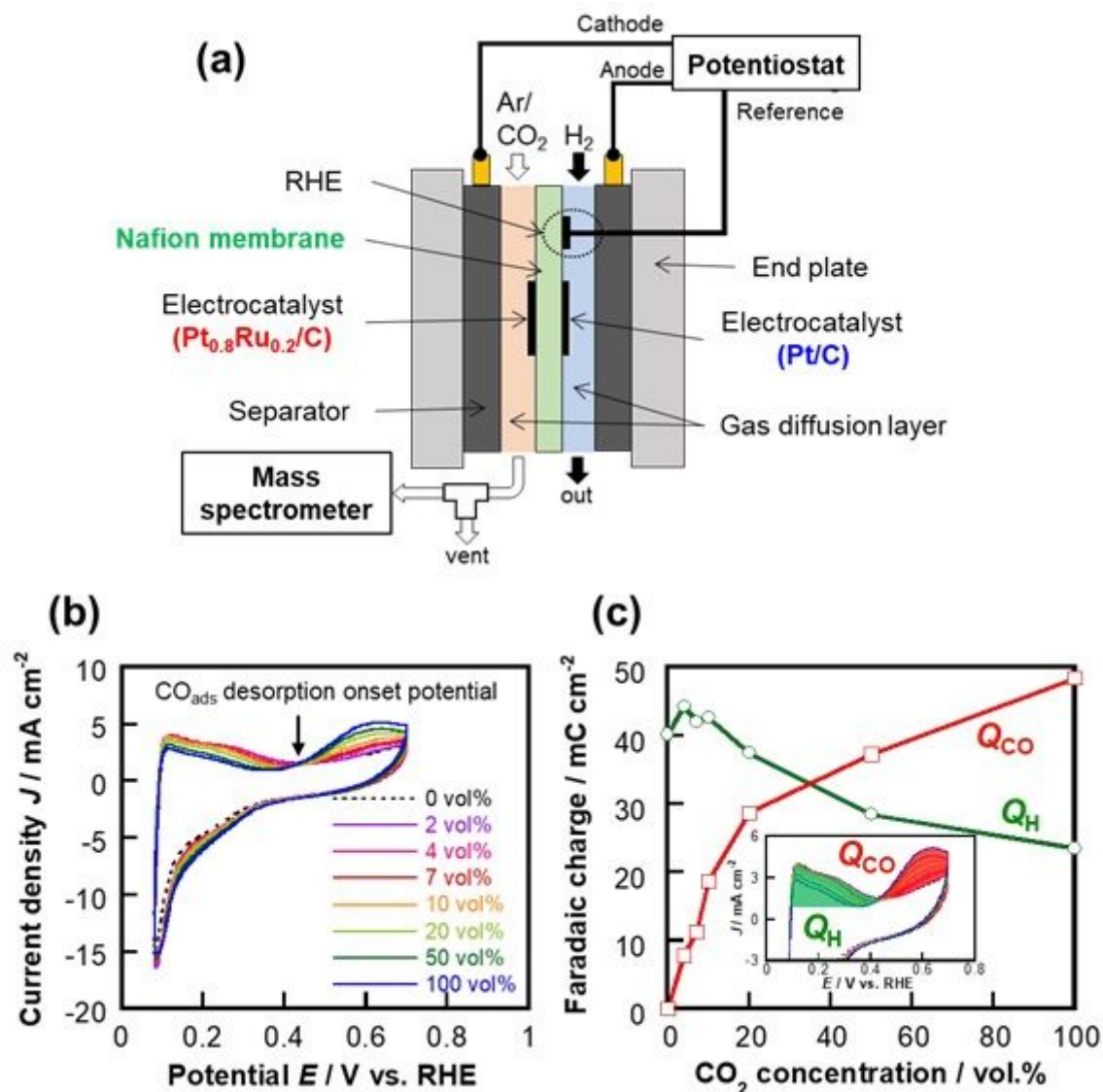


Figure 1

Schematic diagram and performance data. (a) Schematic diagram of the experimental setup used in this study. (b) Cathodic cyclic voltammograms at various concentrations of CO₂ in Ar. (c) CO₂-concentration-dependences of the faradaic charges of the oxidation-current peaks between 0.08–0.43 V (QH) and between 0.43–0.70 V (QCO) (vs. RHE) in the voltammograms shown in (b). The method used to calculate QH and QCO is shown in the inset in panel (c).

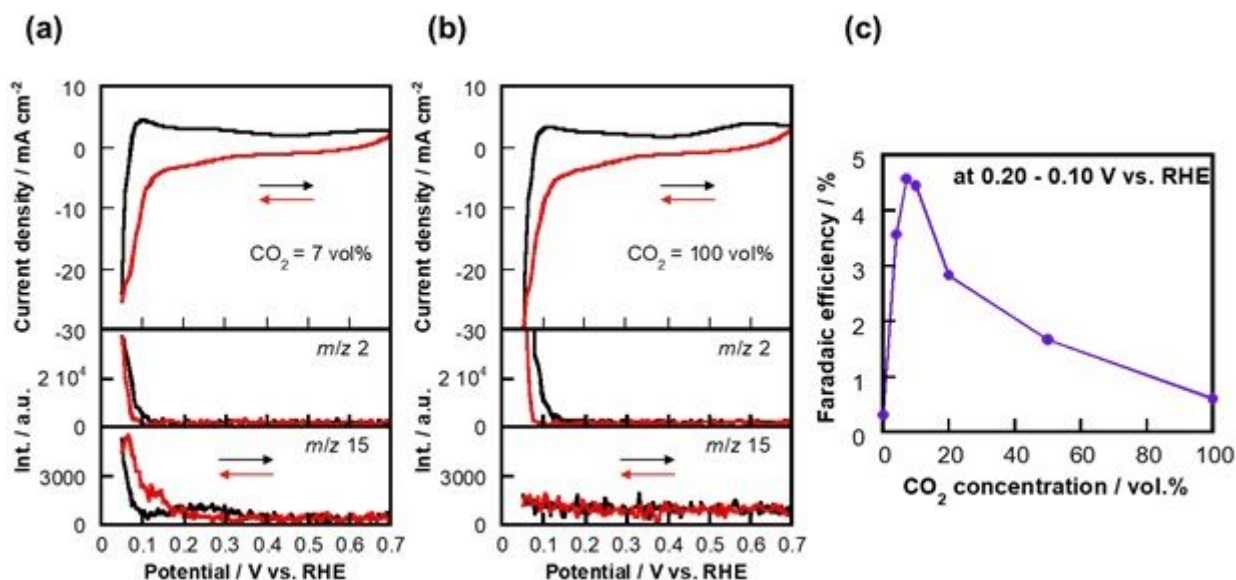


Figure 2

Cyclic voltammetry coupled with mass spectrometry. In-line m/z 2 (for H_2) and 15 (for CH_4) MS signals during CV at CO_2 concentrations of: (a) 7 vol% and (b) 100 vol%. (c) Faradaic efficiency for the generation of CH_4 as a function of CO_2 concentration calculated by integrating the m/z 15-signals in the 0.20–0.10 V (vs. RHE) potential range during negative-scan CV.

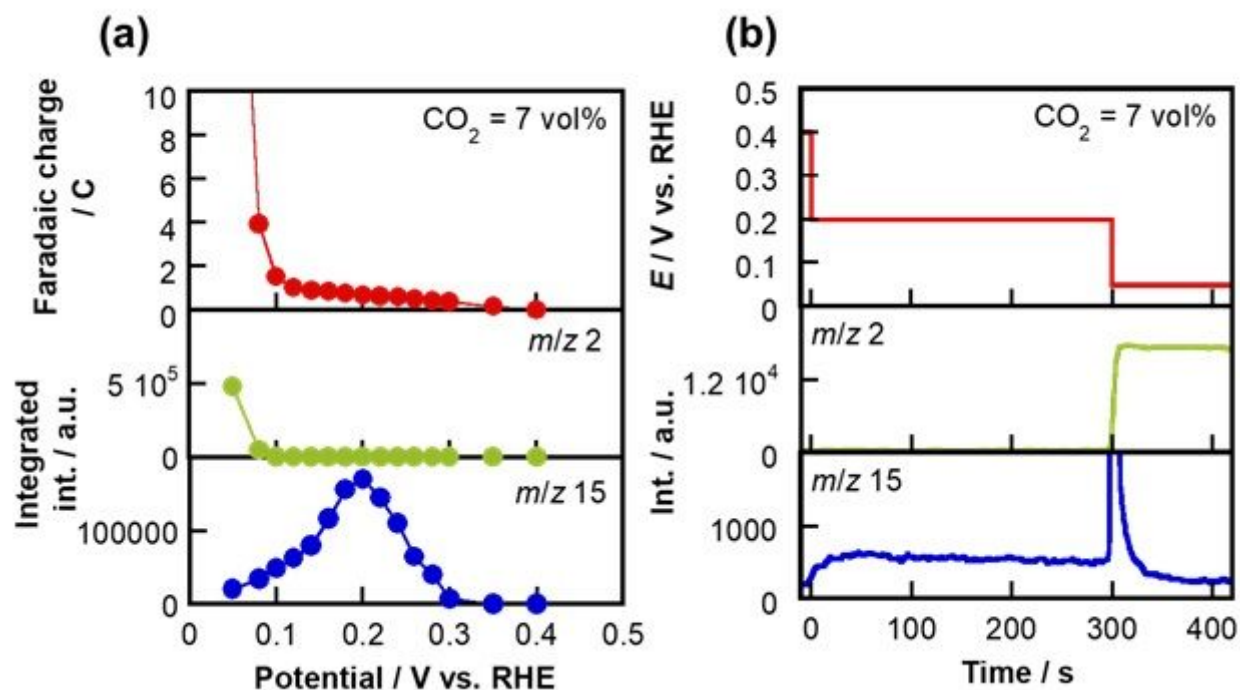


Figure 3

Stationary-potential CO_2 reduction. (a) Potential dependence of faradaic charge, and integrated m/z 2 and 15 MS signals when held at each potential for 2 min at a CO_2 concentration of 7 vol%. (b) Potential program applied to the cathode (upper) and in-line m/z 2 and 15 MS signals (lower) at 7 vol% CO_2 .

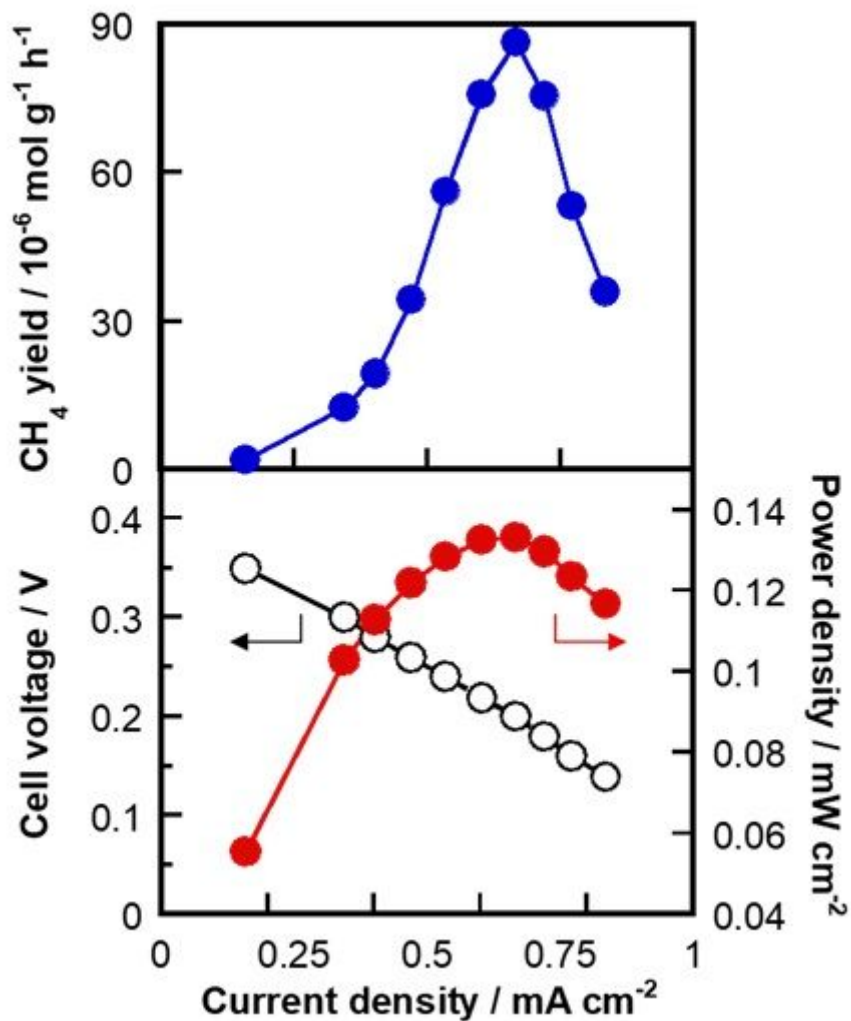


Figure 4

Cell performance. CH₄ yield, cell voltage, and power density as functions of current density at a CO₂ concentration of 7 vol%.

Supplementary Files

This is a list of supplementary files associated with this preprint. Click to download.

- [SupplementarySR.docx](#)